The Atmospheric Pressure Capillary Plasma Jet Is Well-Suited to Supply H2O2 for Plasma-Driven Biocatalysis

Dirks, Tim; Stoesser, Davina; Schüttler, Steffen; Hollmann, Frank; Golda, Judith; Bandow, Julia E.

DOI
10.1002/open.202500057

Publication date
2025

Document Version
Final published version

Published in
ChemistryOpen

ChemistryOpen

Research Article
doi.org/10.1002/open.202500057

Chemistry Europe
European Chemical Societies Publishing

www.chemistryopen.org

The Atmospheric Pressure Capillary Plasma Jet Is Well-Suited to Supply H_2O_2 for Plasma-Driven Biocatalysis

Tim Dirks, Davina Stoesser, Steffen Schüttler, Frank Hollmann, Judith Golda, and Julia E. Bandow*

Plasma-generated H_2O_2 can be used to fuel biocatalytic reactions that require H_2O_2 as a cosubstrate, such as the conversion of ethylbenzene to (*R*)-1-phenylethanol ((*R*)-1-PhOl) catalyzed by unspecific peroxygenase from *Agrocybe aegerita* (r*Aae*UPO). Immobilization is recently shown to protect biocatalysts from inactivation by highly reactive plasma-produced species; however, H_2O_2 supply by the employed plasma sources (μAPPJ and DBD) is limiting for r*Aae*UPO performance. This study evaluates a recently introduced capillary plasma jet for suitability to supply H_2O_2 in situ. H_2O_2 production is modulated by varying the water concentration in the feed gas, providing a greater operating window for applications in plasma-driven biocatalysis. In a static system after 80 min of biocatalysis, a turnover number of 44,199 $mol_{(R)\text{-1-PhOl}}$ $mol^{-1}_{rAaeUPO}$ is achieved without significant enzyme inactivation. By exchanging the reaction solution every 5 min, a total product yield of 122 μmol (*R*)-1-PhOl is achieved in 700 min run time, resulting in a total turnover number of 174,209 $mol_{(R)\text{-1-PhOl}}$ $mol^{-1}_{rAaeUPO}$. This study concludes that the capillary plasma jet, due to its flexibility regarding feed gas, admixtures, and power input, is well suited for in situ H_2O_2 generation for plasma-driven biocatalysis tailoring to enzymes with high H_2O_2 turnover.

1. Introduction

Peroxygenases use hydrogen peroxide to carry out oxyfunctionalization reactions such as stereoselective hydroxylations[1] and epoxidations,[2,3] which are chemically difficult (or impossible) to achieve, making them appealing enzymes for biocatalysis.[4] However, their industrial application is limited since they suffer from hydrogen peroxide-induced inactivation upon disruption of the heme cofactor.[5,6] H_2O_2 levels need to be tightly controlled to not inactivate the biocatalyst. To this end, recently, numerous approaches for in situ H_2O_2 generation have been tested, such as electrochemical,[7,8] photocatalytic,[9,10] and thermoelectric methods[11] or the use of enzyme cascades.[1] Another approach for in situ H_2O_2 generation is the utilization of atmospheric pressure plasmas. These plasmas generate, among many other species, H_2O_2 as a long-living species.[12] A first proof-of-principle study using a dielectric barrier discharge (PlasmaDerm, Cinogy, Germany) as a plasma source revealed that plasma-generated H_2O_2 can be used to drive the reaction of H_2O_2-utilizing enzymes.[13] This initial study revealed two major limitations, namely enzyme stability under plasma conditions and low H_2O_2 supply by that plasma source. Enzyme inactivation is a well-known effect of plasma treatments.[14–16] We would like to highlight three mechanisms: 1) the inactivation of cofactors such as heme;[5,6] 2) the modification of amino acid side chains that are involved in catalysis or are crucial for the enzyme structure (especially histidines or cysteines);[15,17] and 3) the degradation of enzymes by cleavage of peptide bonds, which is presumably induced especially by short-living species.[14] To protect enzymes under plasma treatment conditions, immobilization was identified as a promising tool.[18] By immobilizing enzymes on inert carrier materials, an enzyme-free buffer zone is created between the enzyme-loaded beads and the plasma-exposed liquid surface, allowing the highly reactive short-living species to recombine before they could interact with the enzymes. However, the functional groups used to immobilize enzymes on the carrier material have a profound impact on the plasma stability of the biocatalyst.[18,19] In addition to protecting against plasma-induced inactivation, immobilization allows to reuse the enzymes, increasing the overall cost efficiency of the process. To increase H_2O_2 production, the atmospheric pressure plasma jet (μAPPJ) was evaluated as an alternative plasma source.[20] Higher H_2O_2 production was achieved, the treatable volume was increased, and coupling to online biocatalysis was possible. However, a maximum of 25% of the feed gas could be saturated with water since higher admixtures led to the extinction of the plasma. The input power of the

T. Dirks, D. Stoesser, J. E. Bandow
Applied Microbiology
Faculty of Biology and Biotechnology
Ruhr University Bochum
44801 Bochum, Germany
E-mail: julia.bandow@rub.de

S. Schüttler, J. Golda
Plasma Interface Physics
Faculty of Physics and Astronomy
Ruhr University Bochum
44801 Bochum, Germany

F. Hollmann
Department of Biotechnology
Delft University of Technology
2629HZ Delft, The Netherlands

Supporting information for this article is available on the WWW under https://doi.org/10.1002/open.202500057

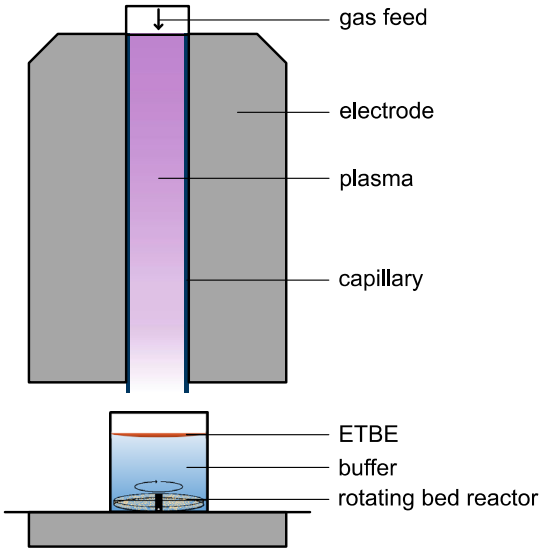

Figure 1. Plasma-driven biocatalysis setup used in this study. The feed gas of the capillary jet was routed through a water-containing bubbler and subsequently guided through a capillary surrounded by two plane-parallel electrodes. The sample, potassium phosphate buffer (5 mL, 100 mM, pH 7) containing 50 mM of the substrate ethylbenzene (ETBE), is exposed to the plasma effluent exiting the capillary. The rotating bed reactor containing the protein-loaded beads is located at the bottom of the vessel. Image was modified from other studies.[13,20,26]

system could not be increased beyond 1.5–2 W, since increasing arc discharges could occur that damage the electrodes.

The H_2O concentration in the feed gas is an important parameter for plasma-induced H_2O_2 generation,[21–25] and H_2O_2 production with the μAPPJ was limited. Thus, in the present study, the capillary plasma jet (CPJ) was used, which allows higher input power and thus higher H_2O concentrations in the feed gas[26] (**Figure 1**). We investigated H_2O_2 formation and biocatalysis performance with the recombinantly produced unspecific peroxygenase from *Agrocybe aegerita* (r*Aae*UPO).[27] Furthermore, we tested alternatives for the amino-functionalized ReliZyme beads (HA403 M) with regard to their utility for plasma-driven biocatalysis.

2. Results and Discussion

Technical, nonthermal atmospheric pressure plasmas can be used as the H_2O_2-producing source to drive the enzymatic reaction of r*Aae*UPO. Previously, the atmospheric pressure plasma jet (μAPPJ) was used for H_2O_2 generation in combination with r*Aae*UPO immobilized on amino-functionalized beads (ReliZyme HA403 M, Resindion),[13,20] resulting in a steady product formation. Owing to a lack of plasma stability at high water vapor admixtures, it was only possible to enrich up to 25% of the feed gas with water. Since the H_2O concentration greatly influences plasma-induced H_2O_2 generation,[21] we tested the performance of the capillary plasma jet[26] in plasma-driven biocatalysis as it enables the use of higher input powers and thus the use of higher H_2O concentrations in the feed gas (100% feed gas routed through the bubbler, 6400 ppm H_2O). Both plasma sources were operated under conditions that allowed the highest H_2O_2 production and H_2O_2 accumulation in the liquid was analyzed (**Figure 2**). As previously observed for the microscale atmospheric pressure plasma jet,[20] the H_2O_2 concentration increased linearly when the CPJ was operated with 100% gas being routed through the bubbler. However, the capillary jet showed H_2O_2 production (based on the linear slope) of 0.14 mM min^{-1}, while the microscale atmospheric pressure plasma jet produced 0.07 mM min^{-1}. The increased H_2O_2 production of the CPJ presumably is caused by the increased amount of H_2O in the feed gas: More water molecules can be dissociated by electron impact dissociation, and more H_2O_2 is generated via the recombination of OH radicals. Furthermore, the higher plasma power of the CPJ leads to increased electron density, which also leads to more dissociation by electron impact dissociation of water molecules.[28]

In plasma-driven biocatalysis, the tailoring of the plasma and thus the amount of H_2O_2 supplied to match the needs and limitations of the enzyme appears very appealing, especially when employing highly H_2O_2-sensitive enzymes in the future. We therefore tested to what extent the H_2O_2 production by the CPJ can be influenced by different H_2O concentrations in the feed gas (**Figure 3**). The range from 50 to 100% feed gas being passed through the bubbler had not been tested to prevent the backflow of H_2O to the mass flow controllers of the plasma source. The H_2O_2 concentration increased drastically upon the introduction of water to the feed gas, showing the importance of H_2O in the feed gas for H_2O_2 production in plasma-treated liquids. H_2O_2 increased from 0.13 mM (0 ppm H_2O) to 0.37 mM (320 ppm H_2O). In the absence of water addition to the gas flow the detected H_2O_2 presumably stems from water contamination. H_2O_2 formation is proportional to the H_2O concentration in the feed gas, and the results are in good agreement with the previously reported measurements for the CPJ.[28] Doubling the H_2O concentration from 320 to 640 ppm led to an increase of H_2O_2 from 0.37 to 0.46 mM. Likely, this is attributable to a certain fraction of the formed H_2O_2 being degraded again in the gas phase.

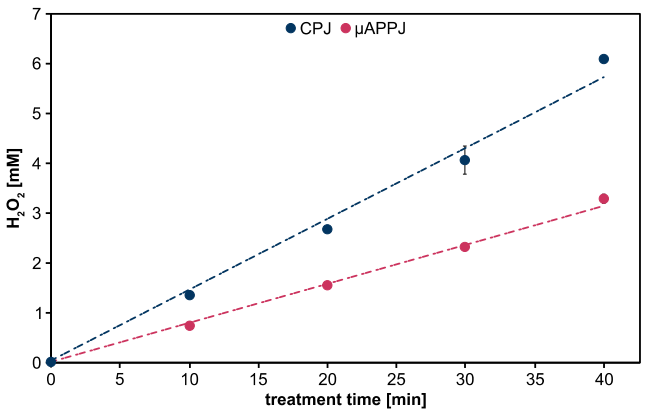

Figure 2. Time-dependent H_2O_2 production. Potassium phosphate buffer (5 mL, 100 mM, pH 7) was treated either with the CPJ and 6400 ppm water in the feed gas or the microscale atmospheric pressure plasma jet (μAPPJ) and 5750 ppm water in the feed gas for up to 40 min. The distance between the nozzle of the jet and the sample was ≈16 mm (CPJ) and 6 mm (μAPPJ). Means and standard deviations reflect three experiments. Standard deviations that are not visible were below 0.1 mM.

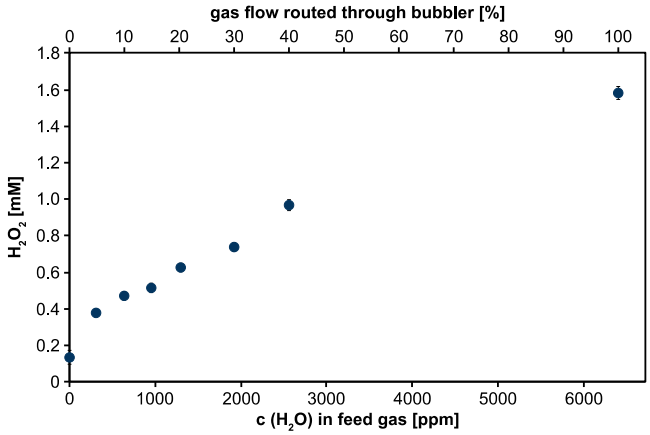

Figure 3. H_2O_2 production at different water concentrations in the feed gas. The feed gas of the capillary jet was (partially) routed through a cooled water-containing bubbler (in %) resulting in different concentrations of water (in ppm) in the feed gas. Potassium phosphate buffer (5 mL, 100 mM, pH 7) was treated for 10 min and the H_2O_2 concentration (in mM) was determined consecutively. Means and standard deviations represent three experiments shown. Standard deviations that are not visible were below 0.01 mM.

The maximum H_2O_2 concentration of 1.6 mM was reached at 10 min treatment time with 6400 ppm H_2O in the feed gas, which equals 100% feed gas routed through the bubbler). This presents a great working range to adjust H_2O_2 production levels to the biocatalyst's needs.

Using the CPJ with maximum water feed for plasma-driven biocatalysis, we tested the (*R*)-1-PhOl production using r*Aae*UPO immobilized on amino-functionalized ReliZyme beads (HA403 M) previously used for studying performance of the μAPPJ,[20] as well as other ReliZyme beads (EA403 M, EP403 M, HFA403 M, BU403 M). Only for the HA304 M and the EA403 M beads considerable product formation was observed (**Figure 4**, data for EP403 M, HFA403 M, and BU403 M are displayed in Supporting Information Figures S1–S3). Importantly, as observed previously for substrate conversion with H_2O_2 generated with the microscale atmospheric pressure plasma jet,[13,20] no substrate degradation or side products were observed in biocatalysis fueled with H_2O_2 generated by the CPJ (Supporting Information Figure S4). Product formation within the tested 40 min run time was comparable between both bead types (HA403 M and EA403 M) and reached a product concentration of ≈1.7 mM (*R*)-1-PhOl (Figure 4). The turnover number for this system was 32,264 $mol_{(R)\text{-1-PhOl}}$ $mol^{-1}_{r\mathit{Aae}UPO}$ for HA403 M and 25,261 $mol_{(R)\text{-1-PhOl}}$ $mol^{-1}_{r\mathit{Aae}UPO}$ for EA403 M, which is in the same range as previously published results obtained using the μAPPJ and plasma-independent methods for H_2O_2 production (Supporting Information Table S1 and S2).[20,29–31] On both bead types, enzyme inactivation was at 10%, and thus residual activity was still very high (Supporting Information Figure S5), indicating that the turnover number might be increased by prolonging the run time of the reaction. This experiment showed that not all beads are equally suited for plasma-driven biocatalysis with r*Aae*UPO.

In a previous study, r*Aae*UPO immobilized on resin-based carriers (Purolite) showed promising activity and plasma tolerance. Especially amino- and epoxy-butyl-functionalized beads showed a high level of plasma protection.[18,19] The Purolite carriers were also tested for their potential use in plasma-driven biocatalysis with the CPJ (**Figure 5**). r*Aae*UPO immobilized on amino-functionalized resin ECR8309F showed comparable product formation to the enzyme on both ReliZyme beads, reaching a product concentration of 1.7 $mM_{(R)\text{-1-PhOl}}$. The r*Aae*UPO on epoxy-butyl-functionalizedresin ECR8285 only reached a product concentration of 1.0 $mM_{(R)\text{-1-PhOl}}$. Using the Purolite beads, we were able to obtain turnover numbers of 32,708 $mol_{(R)\text{-1-PhOl}}$ $mol^{-1}_{r\mathit{Aae}UPO}$ (ECR8309F) and 20,338 $mol_{(R)\text{-1-PhOl}}$ $mol^{-1}_{r\mathit{Aae}UPO}$ (ECR8285), respectively. Maximum conversion rates were calculated from the initial linear slope of the reaction. They were similar for enzymes immobilized on either of the three amino-functionalized beads

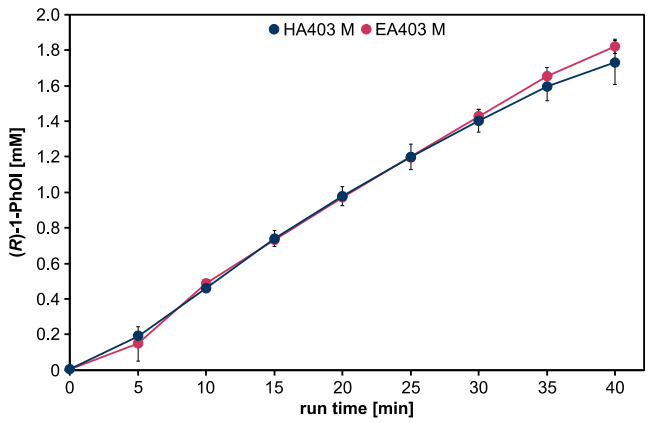

Figure 4. Plasma-driven biocatalysis with the CPJ using rAaeUPO immobilized on ReliZyme beads. Conversion of the substrate ETBE utilized H_2O_2 from direct plasma treatment of the r*Aae*UPO immobilized on ReliZyme HA403 M or EA403 M. Reaction solution contained 5 mL potassium phosphate buffer (100 mM, pH 7) with 50 mM ETBE. Plasma treatment was performed using the CPJ as described above, with a water concentration of 6400 ppm in the feed gas at 6 W plasma power. Every 5 min, aliquots were withdrawn for product analysis by gas chromatography (GC). Means and standard deviations reflect three experiments.

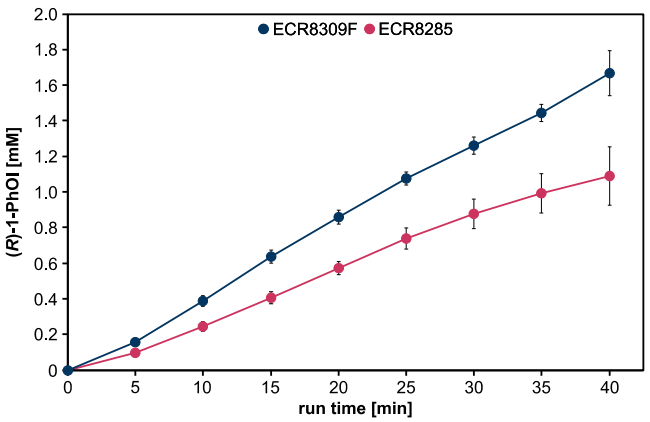

Figure 5. Plasma-driven biocatalysis with the CPJ and r*Aae*UPO immobilized on Purolite beads. The substrate ETBE was converted by r*Aae*UPO immobilized on Purolite ECR8309F and ECR8285. The reaction solution contained 5 mL potassium phosphate buffer (100 mM, pH 7) with 50 mM ETBE. H_2O_2 was generated by plasma treatment with the CPJ and a water concentration of 6400 ppm in the feed gas at 6 W plasma power. Every 5 min aliquots were withdrawn for product analysis by GC. Means and standard deviations represent three experiments.

(≈50 $\mu M_{(R)\text{-1-PhOl}}$ min^{-1}), while the conversion rate for the enzyme on the epoxy-butyl beads was only 30 μM min^{-1} (Supporting Information Table S5). The residual activity after 40 min of biocatalysis at both Purolite carriers decreased to 53% and 17% for ECR8309F and ECR8285, respectively, and thus was lower than for the ReliZyme beads (Supporting Information Figure S5). Weighting conversion rates and enzyme inactivation, the two ReliZyme bead types appear to be the more promising support materials under plasma-operating conditions.

Since for the ReliZyme beads enzyme inactivation after 40 min biocatalysis was negligible, the experiment was repeated, increasing the run time to 80 min (**Figure 6**). After 40 min, for both bead types, product formation rates began to decrease, reaching a plateau at ≈2.3 $mM_{(R)\text{-1-PhOl}}$ after 60 min. Investigation of the residual activity after biocatalysis revealed substantial enzyme inactivation (Supporting Information Figure S6). Substrate conversion decelerated with increasing run times, likely due to the concentration-dependent increasing product inhibition resulting in H_2O_2 accumulation, which we presume is the main cause of enzyme inactivation in this system.[5,6] This notion is supported by the fact that after 80 min of biocatalysis with H_2O_2 provided by the CPJ, the residual enzyme activity was still at ≈35–40% while no more turnover was observed between 70 and 80 min of the biocatalytic reaction. In addition to product inhibition, substrate limitation could also play a role in limiting the reaction at this point (70–80 min). Owing to the poor solubility of ethylbenzene (ETBE), it forms droplets on top of the aqueous reaction solution. There it is exposed to the constant gas flow hitting the surface of the reaction solution, which leads to high substrate evaporation rates and resulting substrate limitation as described previously.[20] Despite the reduced efficiency of biocatalysis during the prolonged run time, it was possible to increase the turnover number to 44,199 $mol_{(R)\text{-1-PhOl}}$ $mol^{-1}_{rAaeUPO}$ (HA403 M) and 34,097 $mol_{(R)\text{-1-PhOl}}$ $mol^{-1}_{rAaeUPO}$ (EA403 M) using the CPJ, respectively (Table S1 and S2, Supporting Information).

For plasma-driven biocatalysis, the turnover number achieved with r*Aae*UPO immobilized on HA403 M beads and replacing the entire buffer system every 10 min was 36,414 $mol_{(R)\text{-1-PhOl}}$ $mol^{-1}_{rAaeUPO}$.[20] In the present study, the same efficiency of plasma-driven biocatalysis was reached without having to replace the reaction solution.

To circumvent the limitations of product inhibition and substrate limitation by periodically removing product and resupplying substrate, a long-term experiment was carried out in which the r*Aae*UPO was immobilized on HA403 M beads and the reaction solution was replaced every 5 or 10 min (**Figure 7**). At a product formation per minute below 0.05 μmol min^{-1}, the enzyme was considered inactive and the reaction was stopped. Using a water vapor concentration of 6400 ppm combined with a reaction solution exchange every 10 min, product formation rates between 0.25 and 0.3 μmol (*R*)-1-Phol min^{-1} were observed in the first 2 h of biocatalysis. Afterward, activity decreased rapidly to 0.15 μmol min^{-1} after 200 min and 0.08 μmol min^{-1} after 400 min, and the biocatalytic reaction was stopped after 500 min run time. Based on the H_2O_2 generation data shown in Figure 3, it is known that using a water concentration of 6400 ppm in the feed gas results in the generation of ≈1.6 mM H_2O_2 in 10 min, which corresponds to 0.8 μmol H_2O_2 min^{-1}. Thus, at the maximum conversion rate of the enzyme, only half of the generated H_2O_2 was converted into (*R*)-1-PhOl. This likely resulted in an excess of H_2O_2 (theoretically of several μmol) within 10 min incubation in one buffer solution. Thus, we assume that the rapid loss of activity after 120 min run time is due to H_2O_2-induced inactivation of r*Aae*UPO. To minimize enzyme incubation in H_2O_2-excess conditions, we considered different strategies to reduce H_2O_2 accumulation, such as increasing the enzyme concentration or scaling up the reaction volume. However, the current reaction setup had technical constraints, particularly the reactor geometry and reaction vessel, that limited the amount of beads (and thus enzyme) and the reaction volume. Since the primary aim of the study was to perform a proof-of-principle experiment to assess the potential for prolonging enzyme

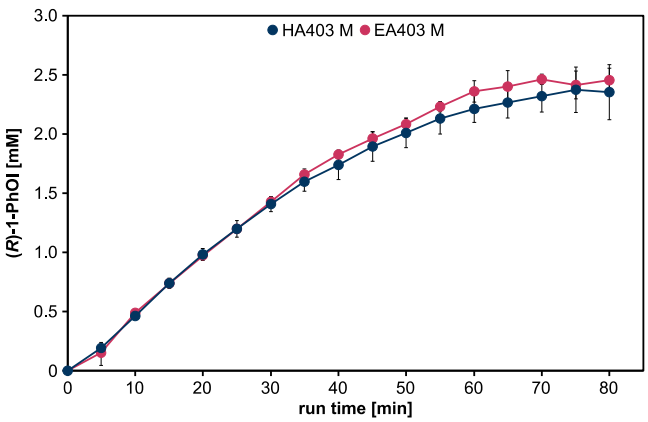

Figure 6. Prolonged plasma-driven biocatalysis with CPJ. Conversion of the substrate ETBE and H_2O_2 from plasma treatment by r*Aae*UPO immobilized on ReliZyme HA403 M and EA403 M was performed as described above, with the CPJ and a water concentration of 6400 ppm in the feed gas at 6 W plasma power. Every 5 min aliquots were withdrawn for product quantification by GC. Means and standard deviations reflect three experiments.

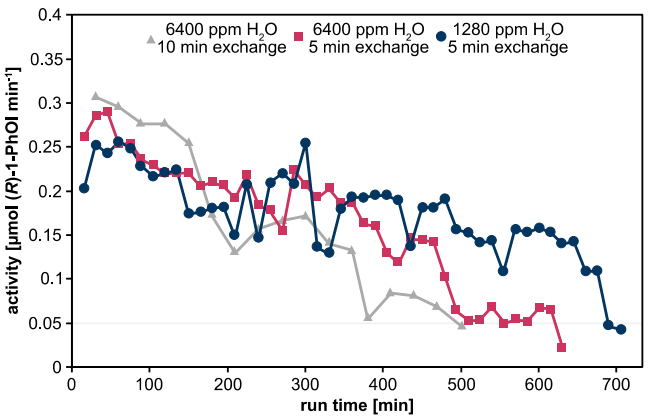

Figure 7. Product formation per minute in long-term experiments with frequent exchange of reaction solutions. Activity of r*Aae*UPO immobilized on HA403 M beads is shown as a function of plasma-driven biocatalysis run time. Every 10 or 5 min, the complete reaction solution was exchanged, and product formation was analyzed by GC measurement. Either 1280 ppm or 6400 ppm H_2O were added to the feed gas to modulate H_2O_2 generation. Means reflect two experiments. A detailed presentation including standard deviations for each experimental condition is provided in the supplements (Supporting Information Figure S7–S9).

lifetime and performance consistency, we reduced the operating time between the reaction solution exchanges to 5 min, moving toward a continuously operated biocatalysis. The reduction of the buffer exchange time resulted in a stabilized production range of 0.17−0.25 μmol (*R*)-1-PhoI per cycle for 460 min. For the 5 min exchange condition, reaction was stopped after 630 min. Thus, stable enzyme performance was extended from 120 to 480 min. Since a more frequent buffer exchange positively affected r*Aae*UPO activity, the experiment was repeated with less H_2O in the feed gas to limit the potential H_2O_2 excess. Based on the maximum conversion rate of ethylbenzene of 0.3 μmol min^{-1}, a water vapor admixture of 1280 ppm to the feed gas was chosen, 0.3 μmol min^{-1} H_2O_2 (see Figure 3). Product formation under these conditions averaged about 0.2 μmol min^{-1} (Figure 7). The activity of the r*Aae*UPO remained above 0.1 μmol (*R*)-1-PhoI min^{-1} until a treatment time of 675 min was reached. The reaction was stopped after 705 min. Inactivation is likely still attributable to an H_2O_2 excess since not all the 0.3 μmol H_2O_2 min^{-1} generated in the cycle were converted, and further reduction in H_2O_2 could positively affect the enzyme lifetime of r*Aae*UPO. This highlights that tailoring of plasma conditions can go a long way to accommodating the requirements of the enzyme.

In addition to activity over time, the total amount of product accumulated over time was analyzed (**Figure 8**). The fastest product increase was observed when 6400 ppm H_2O was admixed and the reaction solution was exchanged every 10 min. Reflecting enzyme inactivation over time, the product accumulation rates declined after ≈150 min, and after 230 min. The total amount of product generated was lower compared to the more frequent reaction solution exchange and the admixture of only 1280 ppm H_2O combined with 5 min cycles, respectively. The use of 1280 ppm H_2O in the feed gas led to the slowest increase in the product but gave the highest final yield of 122 $\mu mol_{(R)\text{-1-PhOI}}$, compared to 84 μmol at 6400 ppm H_2O and 10 min cycles and

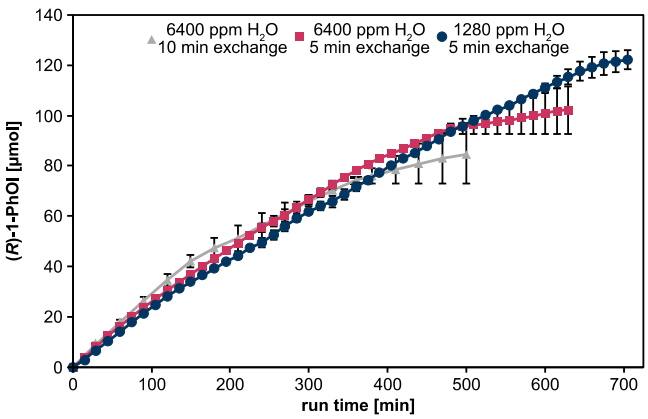

Figure 8. Total product accumulation in the long-term experiment over 5-min or 10-min cycles. Accumulation of generated product (*R*)-1-PhOI produced by r*Aae*UPO immobilized on HA403 M beads after different plasma-driven biocatalysis run times. Either 6400 ppm or 1280 ppm H_2O were added to the feed gas for H_2O_2 generation. Every 10 or 5 min, the complete reaction solution was exchanged, and product formation was analyzed by GC measurement Means and standard deviations representing two experiments are shown. Standard deviations that are not visible were below 2 μmol.

Table 1. Total product formation and TTN calculations of long-term experiment.

Method	Total product [μmol]	TTN [$mol_{(R)\text{-1-PhOI}}$ $mol^{-1}_{rAaeUPO}$]
6400 ppm H_2O, buffer exchange every 10 min	84 ± 12	122 138 ± 5694
6400 ppm H_2O, buffer exchange every 5 min	102 ± 10	138 777 ± 22 687
1280 ppm H_2O, buffer exchange every 5 min	122 ± 4	174 209 ± 3921

102 μmol at 6400 ppm H_2O and 5 min cycles. Accordingly, the highest total turnover number was observed for 1280 ppm H_2O in the feed gas and 5 min cycle times, which was a total turnover number (TTN) of 174,209 $mol_{(R)\text{-1-PhOI}}$ $mol^{-1}_{rAaeUPO}$ (**Table 1**, detailed list for each condition is given in Supporting Information Table S6–S8).

In summary, the turnover number of plasma-driven biocatalysis was increased almost five-fold through the optimization of H_2O_2 production by operating the CPJ with different H_2O admixtures and extending the run time of the process. With a TTN of 174,209 $mol_{(R)\text{-1-PhOI}}$ $mol^{-1}_{rAaeUPO}$, the process of plasma-driven biocatalysis is in the upper range of previously reported total turnover numbers of *Aae*UPO-mediated conversion of ETBE with H_2O_2 generated by in situ methods.[7,29–31] While the efficiency of the process can be further optimized by matching enzyme operating parameters and H_2O_2 even more closely and by adjusting the reactor design, these results highlight that plasma-driven biocatalysis is a competitive method when it comes to enzyme-compatible methods of in situ H_2O_2 generation.

3. Experimental Section

Plasma Source

The CPJ used in this study was identified as a promising source for H_2O_2 generation and H_2O_2 transfer into liquid samples.[28] The radio frequency (RF)-driven (13.56 MHz) atmospheric pressure CPJ was used as described before[23] but with inner capillary (Hilgenberg, Germany) dimensions of 4.56 × 0.88 × 100 mm. The electrodes (itec Automation & Laser AG, Germany) had a width and length of 4 and 40 mm, respectively, resulting in a plasma volume of 4 × 0.88 × 40 mm. The wall thickness of the capillary was 0.22 mm, leading to a distance of 1.32 mm between the electrodes. Plasma was operated at a plasma power of (6.0 ± 0.6) W. The gas flow (2 slm He) was split and partially routed through a bubbler with cooled deionized water to enrich the feed gas with water molecules. The distance between the nozzle of the capillary jet and the sample was ≈16 mm, and the plasma zone ended 10 mm in front of the nozzle exit of the capillary.

H_2O_2 Measurement

H_2O_2 produced in the plasma-treated liquid was measured as described elsewhere.[20] In short, 5 mL potassium phosphate buffer (100 mM, pH 7) were exposed to plasma for different treatment times. Samples were diluted to appropriate concentrations using deionized water and mixed with reagents 1 and 2 of the commercially available Spectroquant H_2O_2 kit (Merck, Germany). After 5 min incubation,

absorption was measured at 455 nm. H_2O_2 concentrations were calculated based on a calibration curve.

Enzyme Preparation and Immobilization

r*Aae*UPO was purified as described previously.[32] For immobilization, two different types of nondirectional carriers were used, namely amino (ECR8309F) and epoxy-butyl (ECR8285) functionalized Lifetech ECR resins (Purolite, Llantrisant, Wales) or amino (HA403 M) ?A3B2 show $146#?>and ethyl-amino (EA403 M) functionalized beads (Resindion, Binasco, Italy). Beads (500 mg) were weighed in a suitable vessel and washed thrice with 5 mL potassium phosphate buffer (100 mM, pH 7). The amino-functionalized carrier materials were incubated in phosphate buffer containing 0.5% (w/v) glutaraldehyde. After 3 h of incubation, beads were washed thrice with potassium phosphate buffer. Enzyme (2 nmol) was added, and immobilization was allowed to proceed overnight at 8 °C with tubes shaking upside down.

Binding Efficiency

After immobilization, binding efficiency was determined by measuring the remaining enzyme activity in the supernatant using 2,2′-azino-bis(3-ethylbenzothiazoline-6-sulfonic acid) (ABTS) as substrate. r*Aae*UPO (2 nmol) or supernatant was added to 100 mM sodium citrate buffer (pH 5) containing ABTS (5 mM). To start the reaction, an equivalent volume of H_2O_2 (2 mM) was added, and product formation was monitored at 405 nm using a microplate reader (Biotek Epoch, Germany). Final concentrations were 2.5 mM ABTS, 1 mM H_2O_2, and 50 mM citrate. Unimmobilized r*Aae*UPO served as control.

Biocatalysis Setup

Plasma-driven biocatalysis was performed as described previously.[20] In short, 150 mg protein-loaded beads were transferred to a rotating bed reactor (build in-house, dimensions: ∅ 2 cm × 0.7 cm). The reactor was placed in a vessel filled with 5 mL potassium phosphate buffer (100 mM, pH 7) containing 50 mM ethylbenzene (ETBE). Plasma treatment was performed for up to 40 min, while every 5 min 150 μL samples were withdrawn for gas chromatography-based quantification of the product as described elsewhere.[13,20] After biocatalysis, residual activity of protein-loaded beads was determined. To this end, beads were recovered from the rotating bed reactor and washed thrice with potassium phosphate buffer. Enzyme activity was determined as described for the unimmobilized enzyme but in a total volume of 1 mL. To ensure sufficient substrate supply, samples were incubated by shaking during turnover. For a total of 10 min reaction time, every 2 min aliquots of 100 μL were removed and measured at a wavelength of 405 nm using a microplate reader (Biotek Epoch, Germany). Enzyme activity was calculated based on the linear slope of the kinetic.

Determination of the Total Turnover Number

For the long-term biocatalysis, 400 mg protein-loaded beads were transferred to a rotating bed reactor. To avoid H_2O_2 accumulation and product inhibition, the entire reaction solution was withdrawn and replaced with fresh solution every 5 or 10 min as indicated. Product formation was analyzed by gas chromatography (GC). After the addition of the fresh potassium phosphate ETBE mixture, plasma treatment was continued. Residual enzyme activity was measured at various time points, and plasma treatment was applied until product formation per minute was below 0.05 μmol min^{-1}.

Conflict of Interest

The authors declare no conflict of interest.

Author Contributions

Tim Dirks: conceptualization, formal analysis, investigation, visualization, writing of original draft. **Davina Stoesser**: investigation. **Steffen Schüttler**: resources, writing—review and editing. **Frank Hollmann**: resources, writing—review and editing. **Judith Golda**: resources, writing—review and editing. **Julia E. Bandow**: conceptualization, funding acquisition, supervision, writing—review and editing.

Data Availability Statement

Additional data are available in the Supporting Information file. All data shown in the manuscript has been deposited to the Research Data Repository and can be accessed using the following link: https://rdpcidat.rub.de/dataset/atmospheric-pressure-capillary-plasma-jet-well-suited-supply-h2o2-plasma-driven-biocatalysis.

Keywords: cold atmospheric pressure plasma jets · gas chromatography · hydroxylations · immobilization · unspecific peroxygenases

[1] Y. Ni, E. Fernández-Fueyo, A. G. Baraibar, R. Ullrich, M. Hofrichter, H. Yanase, M. Alcalde, W. J. H. van Berkel, F. Hollmann, *Angew. Chem., Int. Ed.* **2016**, *55*, 798.
[2] J. Carro, A. González-Benjumea, E. Fernández-Fueyo, C. Aranda, V. Guallar, A. Gutiérrez, A. T. Martínez, *ACS Catal.* **2019**, *9*, 6234.
[3] M. C. R. Rauch, F. Tieves, C. E. Paul, I. W. C. E. Arends, M. Alcalde, F. Hollmann, *ChemCatChem* **2019**, *11*, 4519.
[4] Y. Wang, D. Lan, R. Durrani, F. Hollmann, *Curr. Opin. Chem. Biol.* **2017**, *37*, 1.
[5] B. O. Burek, S. Bormann, F. Hollmann, J. Z. Bloh, D. Holtmann, *Green Chem.* **2019**, *21*, 3232.
[6] A. Karich, K. Scheibner, R. Ullrich, M. Hofrichter, *J. Mol. Catal., B* **2016**, *134*, 238.
[7] A. E. W. Horst, S. Bormann, J. Meyer, M. Steinhagen, R. Ludwig, A. Drews, M. Ansorge-Schumacher, D. Holtmann, *J. Mol. Catal., B* **2016**, *133*, 137.
[8] S. Bormann, D. Hertweck, S. Schneider, J. Z. Bloh, R. Ulber, A. C. Spiess, D. Holtmann, *Biotechnol. Bioeng.* **2021**, *118*, 7.
[9] B. O. Burek, S. R. de Boer, F. Tieves, W. Zhang, M. van Schie, S. Bormann, M. Alcalde, D. Holtmann, F. Hollmann, D. W. Bahnemann, J. Z. Bloh, *ChemCatChem* **2019**, *11*, 3093.
[10] Q. Shen, C. Zhang, L. Chen, B. Huang, Y. Yu, Z. Zhang, W. Zhang, *ACS Sustain. Chem. Eng.* **2022**, *10*, 12156.
[11] J. Yoon, H. Jang, M.-W. Oh, T. Hilberath, F. Hollmann, Y. S. Jung, C. B. Park, *Nat. Commun.* **2022**, *13*, 3741.
[12] P. J. Bruggeman, M. J. Kushner, B. R. Locke, J. G. E. Gardeniers, W. G. Graham, D. B. Graves, R. C. H. M. Hofman-Caris, D. Maric, J. P. Reid, E. Ceriani, D. F. Rivas, J. E. Foster, S. C. Garrick, Y. Gorbanev, S. Hamaguchi, F. Iza, H. Jablonowski, E. Klimova, J. Kolb, F. Krcma, P. Lukes, Z. Machala, I. Marinov, D. Mariotti, S. M. Thagard, D. Minakata, E. C. Neyts, J. Pawlat, Z. L. Petrović, R. Pflieger, et al., *Plasma Sources Sci. Technol.* **2016**, *25*, 053002.
[13] A. Yayci, Á.G. Baraibar, M. Krewing, E. F. Fueyo, F. Hollmann, M. Alcalde, R. Kourist, J. E. Bandow, *ChemSusChem* **2020**, *13*, 2072.
[14] M. Krewing, B. Schubert, J. E. Bandow, *Plasma Chem. Plasma Process.* **2019**, *40*, 685.

[15] J.-W. Lackmann, S. Baldus, E. Steinborn, E. Edengeiser, F. Kogelheide, S. Langklotz, S. Schneider, L. I. O. Leichert, J. Benedikt, P. Awakowicz, J. E. Bandow, *J. Phys. D: Appl. Phys.* **2015**, *48*, 494003.
[16] J.-W. Lackmann, S. Schneider, E. Edengeiser, F. Jarzina, S. Brinckmann, E. Steinborn, M. Havenith, J. Benedikt, J. E. Bandow, *J. Roy. Soc. Interface* **2013**, *10*, 20130591.
[17] M. Krewing, C. K. Jung, E. Dobbelstein, B. Schubert, T. Jacob, J. E. Bandow, *Plasma Process. Polym.* **2020**, *17*, 2000019.
[18] A. Yayci, T. Dirks, F. Kogelheide, M. Alcalde, F. Hollmann, P. Awakowicz, J. E. Bandow, *J. Phys. D: Appl. Phys.* **2021**, *54*, 035204.
[19] T. Dirks, A. Yayci, S. Klopsch, M. Krewing, W. Zhang, F. Hollmann, J. E. Bandow, *J. R. Soc. Interface* **2023**, *20*, 20230299.
[20] A. Yayci, T. Dirks, F. Kogelheide, M. Alcalde, F. Hollmann, P. Awakowicz, J. E. Bandow, *ChemCatChem* **2020**, *12*, 5893.
[21] J. Benedikt, D. Schröder, S. Schneider, G. Willems, A. Pajdarová, J. Vlček, V. S. der Gathen, *Plasma Sources Sci. Technol.* **2016**, *25*, 045013.
[22] C. A. Vasko, D. X. Liu, E. M. van Veldhuizen, F. Iza, P. J. Bruggeman, *Plasma Chem. Plasma Process.* **2014**, *34*, 1081.
[23] J. Winter, H. Tresp, M. U. Hammer, S. Iseni, S. Kupsch, A. Schmidt-Bleker, K. Wende, M. Dünnbier, K. Masur, K.-D. Weltmann, *J. Phys. D: Appl. Phys.* **2014**, *47*, 285401.
[24] G. Willems, J. Benedikt, A. von Keudell, *J. Phys. D: Appl. Phys.* **2017**, *50*, 335204.
[25] Y. Gorbanev, C. C. W. Verlackt, S. Tinck, E. Tuenter, K. Foubert, P. Cos, A. Bogaerts, *Phys. Chem. Chem. Phys.* **2018**, *20*, 2797.
[26] T. Winzer, D. Steuer, S. Schüttler, N. Blosczyk, J. Benedikt, J. Golda, *J. Appl. Phys.* **2022**, *132*, 183301.
[27] P. Molina-Espeja, E. Garcia-Ruiz, D. Gonazlez-Perez, R. Ullrich, M. Hofrichter, M. Alcalde, *Appl. Environ. Microbiol.* **2014**, *80*, 3496.
[28] S. Schüttler, A. L. Schöne, E. Jeß, A. R. Gibson, J. Golda, *Phys Chem. Chem. Phys.* **2024**, *26*, 8255.
[29] F. Tieves, S. J. P. Willot, M. M. C. H. van Schie, M. C. R. Rauch, S. H. H. Younes, W. Zhang, J. Dong, P. G. de Santos, J. M. Robbins, B. Bommarius, M. Alcalde, A. S. Bommarius, F. Hollmann, *Angew. Chem., Int. Ed.* **2019**, *58*, 7873.
[30] W. Zhang, B. O. Burek, E. Fernández-Fueyo, M. Alcalde, J. Z. Bloh, F. Hollmann, *Angew. Chem., Int. Ed.* **2017**, *56*, 15451.
[31] S. J.-P. Willot, E. Fernández-Fueyo, F. Tieves, M. Pesic, M. Alcalde, I. W. C. E. Arends, C. B. Park, F. Hollmann, *ACS Catal.* **2018**, *9*, 890.
[32] P. Molina-Espeja, S. Ma, D. M. Mate, R. Ludwig, M. Alcalde, *Enzyme Microb. Technol.* **2015**, *73*, 29.

Manuscript received: February 3, 2025
Revised manuscript received: May 21, 2025
Version of record online: June 23, 2025